

## Linking of Oligoesters Hydrolysis to Polyurethane Coatings

Mayela Ramirez, Kent R. Miller, Mark D. Soucek

Department of Polymer Engineering, University of Akron, Akron, Ohio 44325

Correspondence to: M. D. Soucek (E-mail: msoucek@uakron.edu)

**ABSTRACT:** The hydrolytic stability of a series of oligoesters comprised of three and four different monomers was evaluated. The hydroxyl terminal oligoesters were prepared from adipic acid (AA) and isophthalic acid (IPA), with six different diols and one triol, which included: 1,4-butanediol, 1,5-pentanediol, 1,6-hexanediol, neopentyl glycol, 2-methyl-1,3-propanediol, trimethylolpropane, and 2-butene-1,4-diol. The hydroxyl terminated oligoesters were reacted with phenyl isocyanate to form telechelic urethane groups. Hydrolysis rate constants were obtained from plots of acid number vs. time. It was observed that ternary oligoester systems had lower hydrolysis rates than quaternary systems. In addition to investigating the hydrolytic stability of the synthesized oligoesters, polyurethane coatings were produced by reacting the hydroxyl-terminated oligoesters with an aliphatic polyisocyanate (1,6-hexanediisocyanate trimer). Model oligoester hydrolysis was then correlated to the weatherability of a crosslinked polyurethane film. © 2013 Wiley Periodicals, Inc. *J. Appl. Polym. Sci.* **2014**, *131*, 40198.

**KEYWORDS:** coatings; degradation; polyurethanes; polyesters

Received 10 September 2013; accepted 15 November 2013

**DOI:** 10.1002/app.40198

### INTRODUCTION

In the coating industry, polyesters enjoy a good reputation due to their excellent adhesion, flexibility, and good impact, scratch, corrosion, and stain resistance. Polyesters are widely used in coil, can, automotive, and industrial coatings and can be formulated as solvent-borne, high solids, waterborne, and powder coatings. However, the performance of polyesters is affected by the sensitivity of ester groups towards water. Under ambient conditions, esters are the most prone to hydrolysis compared to ureas, urethanes and ethers.<sup>1</sup> During hydrolysis, water molecules attack the ester groups at the carbonyl carbon causing the polymer to break into smaller portions, one with a carboxyl-terminated structure and the other one with a terminal hydroxyl group. Continuous attack of water eventually causes a failure of the mechanical properties of the polyester product.

The study of hydroxyl and carboxyl acid terminated oligoesters is important in order to understand and control the storage stability of polyesters in waterborne resins as it pertains to the autocatalysis of hydrolysis due to the presence of telechelic groups. On the other hand, oligoesters are also used as thermosets by crosslinking end-functional groups with isocyanate, melamine or epoxy groups. However, the predicted performance can be quite different from model compounds because most studies base their experiments on mono- or di-ester samples, as well as hydroxyl- or carboxyl terminated resins.<sup>2-4</sup> Furthermore,

the expected performance of crosslinked polyesters is quite different due to the elimination of end-group functionalities.

One of the main characteristics of polyurethane coatings is resistance to harsh outdoor weathering. Polyurethanes provide a barrier against water, heat, and corrosive components. Therefore, understanding the degradation of polyurethane coatings used in outdoor exposure is of main importance for the coatings industry. Weathering studies of outdoor material are also a powerful tool in estimating product life. Product life estimation is of prime importance due to the financial implications of selling a product that does not meet the long term specifications of end-user applications.

Weathering of coatings can be performed outdoors or in chambers that produce accelerated weathering. Natural outdoor weathering in any site requires long exposure time, which makes testing of product time consuming and expensive. Thus, in order to make degradation studies more cost efficient, the coating industry relies on accelerated weathering. Accelerated weathering refers to the degradation of material by artificial light sources that create accelerated degradation. The main goal in using an accelerated weathering test is to learn well in advance the outdoor performance of a material. Results can be obtained within months instead of waiting years in an outdoor natural setting.

To increase the lifetime of exterior coatings, stabilizing additives such as ultraviolet light absorbers (UVAs) and/or hindered

**Table I.** Reactant Quantities Used for the Synthesis of Oligoesters Containing Adipic Acid and Isophthalic Acid as Common Dibasic Acids

Sample	Adipic acid (AA)		Isophthalic acid (IPA)		Diol 1*		Diol 2**	
	mol	g	mol	g	mol	g	mol	g
AA.IPA.14BD	0.51	75	0.51	85	1.54	139	-	-
AA.IPA.15PeD	0.35	47	0.32	53	0.96	100	-	-
AA.IPA.NPG	0.32	47	0.32	53	0.96	100	-	-
AA.IPA.MPD	0.37	54	0.37	61	1.11	100	-	-
AA.IPA.BED	0.31	45	0.3	50	0.91	80	-	-
AA.IPA.NPG.TMP	0.55	80	0.55	91	0.99	103	0.66	88
AA.IPA.16HD.NPG	0.24	35	0.24	40	0.34	40	0.38	40
AA.IPA.MPD.NPG	0.37	54	0.37	61	0.56	50	0.55	48
AA.IPA.16HD.TMP	0.55	80	0.55	91	0.99	116	0.66	88
AA.IPA.MPD.TMP	0.55	80	0.55	91	0.99	89	0.66	88
AA.IPA.16HD.15PeD	0.81	26	0.18	30	0.25	30	0.29	30
AA.IPA.MPD.16HD	0.37	54	0.37	61	0.56	50	0.55	65
AA.IPA.14BD.BED	0.55	80	0.55	91	0.82	74	0.82	72
AA.IPA.15PeD.BED	0.28	40	0.28	46	0.38	40	0.45	40
AA.IPA.MPD.BED	0.37	54	0.37	61	0.55	50	0.54	48

amine light stabilizers (HALS) are added to the coating's formulation. Previous experiments of accelerated weathering of solvent-borne and waterborne clearcoats (2K acrylates polyurethanes) showed a drop of 13% in gloss retention after 2500 h of exposure for stabilized samples. However, unstabilized samples showed a drop of over 40% after 1500 h. Studies made by Seubert et al.<sup>5</sup> also showed the weathering of stabilized and unstabilized acrylic clearcoats (UV-cured and UV and thermally cured).

The aim of the present work is to investigate the hydrolytic stability of the oligoester segment in polyurethanes using urethane terminated oligoesters as a model. Hydroxyl-terminated oligoesters were prepared using a wide variety of diacids and diols and end-capped with phenyl isocyanate in order to eliminate initial end-group effects.<sup>2-4</sup> The hydrolysis rate of the oligoester was monitored using acid titration. The same oligoesters were used to prepare polyester-urethane films. The degradation behavior of the polyurethane coatings under accelerated weathering conditions (strong acid and weatherometer) were compared to the model urethane oligoesters.

## EXPERIMENTAL

### Materials

Isophthalic acid (IPA) ( $\geq 98.0\%$ ), adipic acid (AA) ( $\geq 99.0\%$ ), 1,4-butanediol (14BD) ( $\geq 98.0\%$ ), 2-methyl-1,3-propanediol (MPD) (99%), trimethylolpropane (TMP) (97%), 2-butene-1,4-diol (BED), reagent grade acetone (99.5%), reagent grade ethanol (99.5%), reagent grade phenolphthalein, dibutyltin oxide (DBTO) (98%), dibutyltin dilaurate (DBTDL) (95%), phenyl isocyanate ( $>98\%$ ), and potassium hydroxide (reagent grade  $\geq 90\%$ ) were purchased from Sigma-Aldrich. The 1,5-pentanediol (15PeD), 1,6-hexanediol (16HD), and neopentyl

glycol (NPG) were obtained from BASF. Hexamethylene-1,6-diisocyanate, an aliphatic polyisocyanate, with the commercial name Desmodur N 3300 was kindly provided by Bayer. All materials were used as received, without further purification. Aluminum mill finish 2024-T3 ( $3 \times 6$  in<sup>2</sup>) panels were obtained from Q-Panel Lab Products.

### Synthesis

The hydroxyl functional oligoesters were prepared in a 500-mL three-neck reaction flask equipped with a mechanical stirrer, a nitrogen purge, a Dean-Stark trap, and a heating mantle. The nitrogen purge was used in order to avoid oxidative degradation and moisture absorption of the materials before and during the reaction. It also facilitated the removal of water and other volatile impurities as the resin molecular weight built up. A transesterification catalyst, dibutyltin oxide (DBTO, 0.4 wt %), was used to reduce the reaction time. Xylene (3 wt %) was added into the flask at the beginning of the reaction. Additionally, the Dean-Stark trap was filled with xylene to the reflux connection to azeotrope water away from the resin.

The reaction temperature was carefully controlled using a Love Controls Series 2600 auto-tuning PID temperature controller and a J-type thermocouple. The temperature was set at 150°C for 30 min, 160°C for 60 min, 195°C for 120 min, and at 210°C for 30 min. The final temperature, 210°C, was maintained until the resin reached an ultimate acid number of less than or equal to 8 mgKOH/gresin. The oligoesters were purified by drying at 110°C for 5 h under vacuum (1 mmHg) to remove the residual xylene and low molecular weight byproducts. The acid number and hydroxyl number of all the oligoesters were measured according to the ASTM standards D 1639-90 and D 4274-99, respectively. Table I lists the reactants and quantities used for each oligoester. Identification of oligoesters was

**Table II.** Formulation of Poly(ester-urethane coatings)

Sample	HDI			Wetting
	Sample weight (g)	Isocyanurate (g)	MEK (g)	Additive (g)
AA.IPA.14BD	8.35	4.79	8.3	0.026
AA.IPA.15PD	8.09	4.65	5.39	0.025
AA.IPA.16HD	7.72	5.35	5.15	0.026
AA.IPA.MPD	9.17	6.8	9.17	0.03
AA.IPA.NPG	7.72	6.6	5.15	0.028
AA.IPA.BED	6.93	3.15	4.62	0.02
AA.IPA.MPD.BED	7.8	4.07	5.2	0.023
AA.IPA.14BD.BED	9.81	4.39	6.54	0.028
AA.IPA.15PD.BED	8.42	7.05	8.42	0.03
AA.IPA.MPD.16HD	8.35	4.73	8.3	0.026
AA.IPA.MPD.NPG	7.6	4.78	5.8	0.024
AA.IPA.MPD.TMP	8.04	4.86	5.36	0.025
AA.IPA.NPG.TMP	7.89	4.77	5.26	0.025
AA.IPA.16HD.TMP	8.86	5.58	5.9	0.028
AA.IPA.16HD.NPG	7.19	4.24	4.79	0.023
AA.IPA.16HD.15PD	5.36	2.5	3.57	0.015

completed using acronyms which start with the dibasic acids followed by the diol(s). For example, AA.IPA.14BD is an oligoester comprised of adipic acid (AA), isophthalic acid (IPA), and 1,4-butanediol (14BD).

Hydroxyl terminated polyesters were then end-capped with phenyl isocyanate (PI). Dibutyltin dilaurate (DBTDL, 0.1 wt %) was used as catalyst to accelerate the reaction. Excess isocyanate was used in order to assure the reaction of all hydroxyl groups. To ensure that all hydroxyl groups were end-capped, an excess ratio of isocyanate to hydroxyl groups was used (1.1 : 1). The reactants were mixed and heated to 100°C. The reaction was monitored by FT-IR and considered complete by the disappearance of the hydroxyl peak and the formation of the carbamate peak. After which, any excess phenyl isocyanate was removed *in vacuo*.

#### Material Characterization

FTIR spectra were measured on a Nicolet-380 spectrometer in the range of 4000–400 cm<sup>-1</sup>. Absorbance spectra were acquired at 4 cm<sup>-1</sup> resolution and the signal was averaged over 32 scans.

Gel Permeation Chromatography measurements were performed on a Waters GPC instrument equipped with a series of six Styragel columns (HR 0.5, HR 1, HR 3, HR 4, HR 5, and HR 6) calibrated with narrow-MWD polystyrene standards. Tetrahydrofuran was used as the mobile phase with a flow rate of 1.0 mL min<sup>-1</sup>. A refractive index (RI) detector (Optilab, Wyatt Technology), a dual-ultraviolet absorbance detector (Waters 2487), and a laser light scattering detector (Minidawn, Wyatt Technology) were used to obtain number average molecular weight (MN), weight average molecular weight ( $M_w$ ), and polydispersity index (PDI).

Glass transition and melting temperatures for all samples were measured on a Q1000 differential scanning calorimeter (DSC) from TA Instruments at a heating rate of 10°C min<sup>-1</sup>. The experiments were run under nitrogen atmosphere.

Viscoelastic properties were measured on a dynamic mechanical thermal analyzer (DMTA V, Rheometrics Scientific, Piscataway, NJ). Stretching mode was used at a frequency of 1 Hz and a heating rate of 3°C min<sup>-1</sup> over a range of -50 to 120°C. The testing conditions and methodology were based on ASTM D 4065-95.75 A minimum preload force of 200 mN was applied by the instrument. The gap distance was arranged at 4 mm for rectangular specimens with the following dimensions: 10 mm of length, 8–10 mm of width, and 0.09–0.11 mm in thickness. When  $T \gg T_g$ , the loss modulus ( $E''$ ) is very low and the modulus ( $E$ ) can be considered approximately equal to the storage modulus ( $E'$ ). Thus, the crosslink density ( $\nu_e$ ) of the films was obtained through the storage modulus in the rubbery plateau region. The relationship between rubbery plateau modulus and crosslink density is given by the following equation:

$$\nu_e = \frac{E'_{\min}}{3RT}$$

where  $\nu_e$  is the crosslink density of elastically effective network chains,  $E'_{\min}$  is the minimum value of the storage modulus (Pa) above  $T_g$ ,  $R$  is the gas law constant, and  $T$  is the temperature.

#### Coating Formulation and Film Preparation

Polyesters were diluted in methyl ethyl ketone (30–50 wt %) and then mixed with hexane-1,6-diisocyanate (HDI isocyanurate). The mole ratio of isocyanate group to hydroxyl group was kept constant at 1.1 : 1. A wetting additive, Tego wet 270, at 0.2 wt % was added into the mixture to achieve even dispersion. All

**Table III.** Test Program Settings of SAE J1960 Used on the Accelerated Weathering of Polyurethane Films

Parameters	SAE J1960
Total number of segments:	4
Duration units (Time/Irrad.)	Irradiance
Controlling black sensor (BPT/BST)	BPT—black panel
Is black temperature active?	Yes
Irradiance filter	340 nm
Chamber (DB) temperature active	Yes
<b>Light Cycle Settings:</b>	
Irradiance (340 nm filter)	0.55 W m <sup>-2</sup>
Black panel temperature	70°C
Chamber (DB) temperature	47°C
Relative humidity	50%
<b>Dark Cycle Settings:</b>	
Chamber (DB) temperature	38°C
Relative humidity	95%
Segment 1	
Cycle	Dark
Duration (minutes/joules)	60 minutes
Specimen spray (on/off)	On
Rack spray (on/off)	On
Segment 2	
Cycle	Light
Duration (minutes/joules)	1320 joules
Specimen spray (on/off)	Off
Rack spray (on/off)	Off
Segment 3	
Cycle	Light
Duration (minutes/joules)	660 joules
Specimen spray (on/off)	On
Rack spray (on/off)	Off
Segment 4	
Cycle	Light
Duration (minutes/joules)	1980 joules
Specimen spray (on/off)	Off
Rack Spray (on/off)	Off

aluminum panels (alloy 3003 H14, Q-panel lab products) were degreased with acetone. The films were cast on the aluminum panels with a drawdown bar with thickness of 150  $\mu\text{m}$  (6 mil). The films were cured at 120°C for 2 h. For mechanical and tensile properties, the films were cast on a glass panel and a drawdown bar of 200  $\mu\text{m}$  (8 mil) was used. The cured films were stored for 3 days under ambient conditions in a dust-free cabinet before testing. Actual formulation amounts of polyesters, solvent, HDI isocyanurate, and additive are given in Table II.

#### Hydrolytic Degradation

Hydrolysis of the oligoesters was performed by titration of the formation of carboxylic acid at different points. Oligoesters were dissolved in acetone, followed by addition of distilled

**Table IV.** Physical Properties of End-Capped Oligoesters

Sample	$M_n$	PDI	$T_g$ (°C)
AA.IPA.14BD	1390	1.39	-22
AA.IPA.15PeD	1360	1.37	-14
AA.IPA.NPG	1390	1.24	-12
AA.IPA.MPD	1180	1.24	-3
AA.IPA.BED	1190	1.4	-18
AA.IPA.NPG.TMP	1900	1.26	-5
AA.IPA.16HD.NPG	1620	1.08	-17
AA.IPA.MPD.NPG	1640	1.31	-9
AA.IPA.16HD.TMP	1920	1.2	-18
AA.IPA.MPD.TMP	1910	1.15	-21
AA.IPA.16HD.15PeD	1020	1.29	-34
AA.IPA.MPD.16HD	1210	1.21	-24
AA.IPA.15PeD.BED	1070	1.18	-14
AA.IPA.MPD.BED	1590	1.08	-15

water and vigorous agitation. Equivalent amounts of oligoester, acetone, and water were used to maintain a large molar excess of water relative to the formation of carboxylic acid of the partially hydrolyzed oligoester. To accelerate the experiment, the solution was sealed and placed in a 40°C constant-temperature water bath. Periodically, an aliquot of the oligoester solution was removed and dried in a convection oven at 110°C for 3 h. After drying, 1 g of the dried resin was dissolved in 25 g of an equal mixture of acetone and ethanol for titration with a 0.1 N solution of potassium hydroxide in methanol to a pink phenolphthalein endpoint. In addition, the reduction in molecular weight was also monitored by gel permeation chromatography. Hydrolysis of polyurethane films was performed at 60°C in a solution of 5.5 N H<sub>2</sub>SO<sub>4</sub>.

#### Accelerated Weathering

Weathering of polyurethane films was completed on a Xenon Arc Weather-Ometer from ATLAS Material Testing Technology LLC model Ci4000. The Weather-Ometer uses a Xenon Arc lamp and has Type "S" Borosilicate inner and outer filters, which is the most common combination for weathering tests. Table III shows the SAE J1960 test program. Four aluminum panels coated with the polyurethane film were exposed for 60 days to the same weathering conditions. Every 20 days a sample was removed from the chamber and the coating properties were measured. The test program was SAE J 1960, which consists of four segments: one dark and three light segments. SAE J1960 exposes samples to more light in the 280–295 nm range than is screened out by the Earth's ozone layer. The strength of this cycle is that it includes a dark cycle with water spray at a lower temperature to simulate nightly condensation and the subsequent drying concurrent with temperature increase during the morning.

#### Film Characterization

The PU films were evaluated by pencil hardness (ASTM D 3363-00), cross-hatch adhesion test (ASTM D 3359-02), pull-off

**Table V.** Relative Hydrolysis Rate Constants for Model End-Capped Oligoesters

Sample	$K'$ (mg <sub>KOH</sub> /g <sub>resin</sub> -day) × 10 <sup>3</sup> ± std. dev.
AA.IPA.14BD	34.4 ± 2.7
AA.IPA.15PeD	37.1 ± 1.2
AA.IPA.NPG	35.1 ± 3.3
AA.IPA.MPD	62.5 ± 3.0
AA.IPA.BED	113.1 ± 5.9
AA.IPA.NPG.TMP	46.5 ± 0.4
AA.IPA.16HD.NPG	54.3 ± 1.3
AA.IPA.MPD.NPG	50.2 ± 1.9
AA.IPA.16HD.TMP	52.8 ± 2.3
AA.IPA.MPD.TMP	41.5 ± 2.5
AA.IPA.16HD.15PeD	57.9 ± 0.6
AA.IPA.MPD.16HD	45.8 ± 6.1
AA.IPA.15PeD.BED	64.1 ± 0.4
AA.IPA.MPD.BED	63.9 ± 1.1

adhesion test evaluates (ASTM D 4541-02)<sup>84</sup>, and gloss (ASTM D 523). Gloss measurements were done with a NOVO-GLOSS instrument (Elcometer 401) at 20°/60° angle, including Novosoft software used to analyze the gloss values. Ten replicates of each test were performed with the average and standard deviation reported.

## RESULTS

In this study, the focus was entirely on the hydrolytic stability of oligoester portion of polyurethanes. It is acknowledged that the weathering of urethanes also include photo-oxidation, however, it was the aim to link an oligoester behavior from model urethane to solid film urethane. In the case of polyesters, two major attributes are considered when formulating polyester products to be used in exterior or harsh environments where water is a constant presence: the steric and the anchimeric effects.<sup>2</sup> Usually, one would like to have the shielding provided by bulky molecules that impede the nucleophilic attack and at the same time provide good mechanical properties. Additionally, the use of small linear monomers that can impart flexibility and low viscosity is also desired. To analyze these two effects, oligoester containing linear and sterically bulky monomers were synthesized to observe the respective impact on the hydrolysis rates. The oligoester were formulated into polyurethane films to determine if similar degradation behavior were observed for the model compounds (end-capped oligoesters) and the polyurethane films synthesized with the hydroxyl-terminated oligoesters and 1,6-hexanediisocyanate isocyanurate (HDI isocyanurate). The films were subjected to an accelerated hydrolysis test via emersion in a strong acid solution. This insures that the dominant degradation pathway was by hydrolysis. Because the PU films were not soluble, hydrolysis rates were obtained by measuring weight loss. To bring a more realistic environment, a neutral pH wet and light cycle was used to evaluate the oligoester behavior. After exposure the films were evaluated

mechanically, IR, and gloss. For gloss measurements, exterior durability additives were added for comparison.

Linear glycols with four to six carbon spacers were chosen for their anchimeric interactions (back-biting mechanism).<sup>6</sup> In addition, linear glycols allowed for the comparison between less hindered and more bulky diols such as neopentyl glycol (NPG) or 2-methyl-1,3-propanediol (MPD).<sup>1</sup> Both the neopentyl glycol (NPG) and trimethylolpropane (TMP) were selected based on the reported hydrolytic stability and common use.<sup>2,6-8</sup> The 2-butene-1,4-diol (BED) was used as an example of a short unsaturated diol.

The selection of weathering cycle was based on previous studies<sup>9-11</sup> that showed that SAE J1960 test with a combination of borosilicate inner and outer filter instead of Quartz/Borosilicate gives a better correlation with solar radiation. Minimizing the UV radiation below 290 nm is of utmost importance because it is part of the UVC range, which is the most destructive to polymers and colorants. In natural weathering, UV radiation below 295 nm is filtered out by the ozone layer. Because the UV light cutoff for the xenon light with borosilicate inner/outer filter is around 290 nm and that for the xenon with quartz/boro inner/outer filter is around 280 nm, this last filter combination was selected for the experiments in this research. Previous studies based on different accelerated weathering tests<sup>10</sup> have shown that accelerated weathering of acrylic coatings with xenon arc artificial light and either set of filters, xenon boro/boro or xenon quartz/boro, correlated well with natural weathering. However, natural weathering of polyester coatings only correlated properly using the borosilicate inner/outer filter. Comparison of cycle also favors SAE J1960 over ASTM G26 (latter known as ASTM G155). The cycle used on the SAE J1960 includes a dark cycle with water spray at low temperatures that simulates a dew point occurring at night.

## Oligoester Properties

The number average molecular weight ( $M_n$ ), polydispersity index (PDI), and the glass transition temperature ( $T_g$ ) for each of the model end-capped oligoesters is shown in Table IV. The relative hydrolysis values for the oligoesters, obtained by monitoring the change in acid number over time are shown in Table V. The highest hydrolysis rate of  $113.1 \pm 5.9$  mg<sub>KOH</sub>/g<sub>resin</sub>-day was obtained by the AA.IPA.BED oligoester followed by the other oligoesters contain BED, AA.IPA.15PeD.BED > AA.IPA.MPD.BED. For the remaining oligoesters, the hydrolysis rate decreased as the aromatic content of the oligoester increased.

The high rates of hydrolysis for the oligoesters containing BED can be explained by Turpin's rule.<sup>6</sup> BED represents the

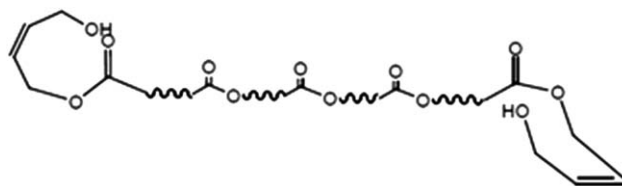


**Figure 1.** End-group effect caused by hydroxyl terminated oligoesters composed of 2-butene-1,4-diol end-groups.

**Table VI.**  $T_g$  and Crosslink Density of PU Films

Sample	$T_g$ ( $^{\circ}\text{C}$ ) from $\tan \delta$	Crosslink density ( $\text{mol m}^{-3}$ )
AA.IPA.14BD	-0.4	109.3
AA.IPA.15PeD	30.5	251.5
AA.IPA.NPG	59.3	101.7
AA.IPA.MPD	43.7	170.7
AA.IPA.BED	19.8	131.1
AA.IPA.NPG.TMP	69.9	51.6
AA.IPA.16HD.NPG	41.1	90.9
AA.IPA.MPD.NPG	44	81.1
AA.IPA.16HD.TMP	45.3	257.1
AA.IPA.MPD.TMP	72.5	152.4
AA.IPA.16HD.15PeD	27.6	166.2
AA.IPA.MPD.16HD	32	564.8
AA.IPA.15PeD.BED	12.7	102.8
AA.IPA.MPD.BED	44	392.9

monomer with the lowest steric factor ( $\text{SF} = 10$ ). Additionally, linear and flexible end-groups can be formed when segments of AA.BED are present in the chain. The low steric hindrance and flexibility of these groups increase the hydrolysis rates through anchimeric effect (inter- and intramolecular catalysis). Low concentration of BED at the chain ends can also contribute to nucleophilic attack. The BED can undergo a back-biting mechanism forming a cyclic structure that locks the oligomers in one position (Figure 1), generating a carbonyl carbon more susceptible to nucleophilic attack.

#### Polyurethane Film Properties

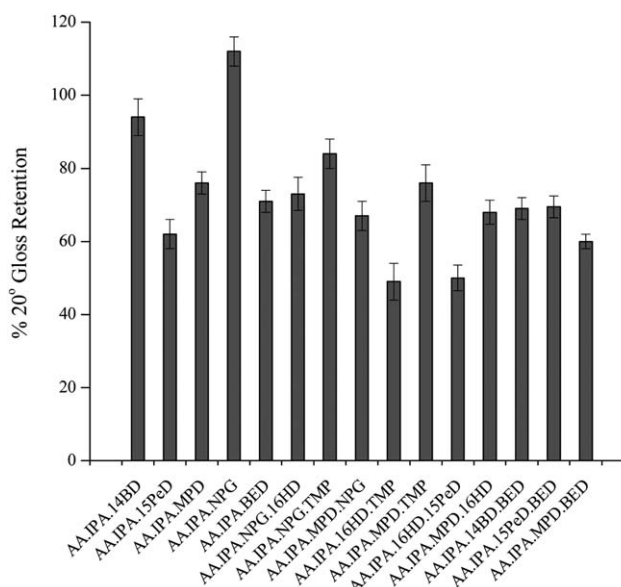
The glass transition temperature ( $T_g$ ) and the crosslink density obtained from DMA analysis for all the polyester-urethane (PU) films are shown in Table VI. PU films containing AA-oligoesters show the lowest  $T_g$ 's compared to other systems.

**Table VII.** Hydrolysis Rate of PU Films

Sample	Weight loss rate ( $\text{mg day}^{-1}$ )
AA.IPA.14BD	$4.17 \pm 0.43$
AA.IPA.15PeD	$6.81 \pm 0.87$
AA.IPA.NPG	$3.41 \pm 0.52$
AA.IPA.MPD	$6.04 \pm 0.84$
AA.IPA.BED	$10.87 \pm 1.44$
AA.IPA.NPG.TMP	$2.62 \pm 0.30$
AA.IPA.16HD.NPG	$3.94 \pm 0.30$
AA.IPA.MPD.NPG	$4.58 \pm 0.04$
AA.IPA.16HD.TMP	$4.76 \pm 0.18$
AA.IPA.MPD.TMP	$2.74 \pm 0.38$
AA.IPA.16HD.15PeD	$3.62 \pm 0.21$
AA.IPA.MPD.16HD	$4.01 \pm 0.59$
AA.IPA.15PeD.BED	$9.03 \pm 0.27$
AA.IPA.MPD.BED	$6.05 \pm 0.62$

The hydrolysis rates of the PU films are shown in Table VII. The hydrolysis rates showed similar trends compared to the end-capped oligoesters. Polyurethane films containing AA.IPA.BED had the highest degradation rates, and the AA.IPA.NPG PU films showed the lowest hydrolysis rates. Polyurethane films of AA.IPA.BED; AA.IPA.1,5-PeD; and AA.IPA.1,6-HD quickly degraded and lost their shape, forming a sticky solid. Polyurethane films with the best hydrolytic stability were AA.IPA.NPG.TMP ( $2.62 \text{ mg day}^{-1}$ ) and AA.IPA.TMP.MPD ( $2.74 \text{ mg day}^{-1}$ ). These films showed different trends compared to the corresponding model compounds. On the other hand, polyurethane films with the worst hydrolytic stability were: AA.IPA.BED ( $10.9 \text{ mg day}^{-1}$ ) > AA.IPA.15PeD.BED ( $9.0 \text{ mg day}^{-1}$ ) > AA.IPA.15PeD ( $6.8 \text{ mg day}^{-1}$ ) > AA.IPA.MPD  $\approx$  AA.IPA.MPD.BED ( $6.0 \text{ mg day}^{-1}$ ).

To observe the changes in the chemical structure during hydrolysis, the FT-IR spectrum of the PU films was obtained before and after hydrolysis. The spectra of all of the samples are similar. Strong absorption bands were observed at  $1680 \text{ cm}^{-1}$  ( $\nu(\text{C}=\text{O})$  stretching of urethane and ester groups),  $1460 \text{ cm}^{-1}$  ( $-\text{CH}-$  deformation of methylene groups),  $1240 \text{ cm}^{-1}$  ( $\nu(\text{C}-\text{N}) + \delta(\text{NH})$ , H-bonded), and  $730 \text{ cm}^{-1}$  (aromatic ring bending mode). Double absorption bands are observed in the range of  $1680\text{--}1720 \text{ cm}^{-1}$ . The band at  $1680 \text{ cm}^{-1}$  is related to the  $\nu(\text{C}=\text{O})$  stretching of H-bonded urethane and ester, and the band at  $1720 \text{ cm}^{-1}$  is related to free carbonyl groups. After hydrolysis, this double band becomes a single absorption peak with a weak shoulder. This shoulder is related to the free carboxyl acid groups that hydrolyzed and washed away during the experiment. Some other bands are observed at  $3390 \text{ cm}^{-1}$  ( $\nu(\text{N}-\text{H})$ ),  $2940 \text{ cm}^{-1}$  ( $\nu(\text{C}-\text{H})$ ),  $1540 \text{ cm}^{-1}$  ( $\nu(\text{C}-\text{N}) + \delta(\text{N}-\text{H})$ , H-bonded and free),  $1140 \text{ cm}^{-1}$  ( $\nu(\text{C}-\text{O}-\text{C})$ ), and  $770 \text{ cm}^{-1}$  (out of plane bending vibration of four adjacent hydrogens on aromatic ring). All these absorptions confirmed polyurethane synthesis.

**Figure 2.** Gloss retention ( $20^{\circ}$ ) of polyurethane films after 1440 h of accelerated weathering.

**Table VIII.** Gouge Hardness Values Obtained During Weathering

PU films	Gouge hardness			
	t = 0 h	t = 480 h	t = 960 h	t = 1440 h
AA.IPA.14BD	6H	5H	5H	5H
AA.IPA.15PeD	6H	4H	4H	5H
AA.IPA.NPG	4H	4H	4H	4H
AA.IPA.MPD	6H	5H	5H	5H
AA.IPA.BED	6H	5H	5H	5H
AA.IPA.NPG.TMP	6H	5H	5H	5H
AA.IPA.16HD.NPG	6H	4H	3H	6H
AA.IPA.MPD.NPG	6H	6H	6H	6H
AA.IPA.16HD.TMP	6H	6H	6H	6H
AA.IPA.MPD.TMP	6H	6H	6H	6H
AA.IPA.16HD.15PeD	6H	2H	HB	HB
AA.IPA.MPD.16HD	6H	5H	6H	6H
AA.IPA.14BD.BED	6H	6H	6H	5H
AA.IPA.15PeD.BED	6H	6H	6H	5H
AA.IPA.MPD.BED	6H	6H	6H	5H

**Weathering of Polyurethane Films**

Accelerated weathering of polyurethane coatings made with different oligoester structures was monitored through gloss retention for a period of 1440 h. Gloss is the physical property most commonly used to follow weathering.<sup>11</sup> Additionally, in the automotive coating industry, gloss loss caused by weathering is of more concern than yellowing. Gloss retention percentage at the end of each experiment was plotted and shown in Figure 2. The results show low weathering performance for the following

**Table IX.** Scratch Hardness Values Obtained During Weathering

PU films	Scratch hardness			
	t = 0 h	t = 480 h	t = 960 h	t = 1440 h
AA.IPA.14BD	5H	4B	6B	HB
AA.IPA.15PeD	5H	4H	2H	2B
AA.IPA.NPG	4H	B	F	F
AA.IPA.MPD	5H	6H	2H	2B
AA.IPA.BED	5H	3H	3H	HB
AA.IPA.NPG.TMP	4H	4H	3H	2H
AA.IPA.16HD.NPG	5H	5H	4H	4H
AA.IPA.MPD.NPG	5H	5H	4H	3H
AA.IPA.16HD.TMP	5H	5H	5H	4H
AA.IPA.MPD.TMP	5H	5H	4H	3H
AA.IPA.16HD.15PeD	3H	F	3B	3B
AA.IPA.MPD.16HD	5H	5H	4H	4H
AA.IPA.14BD.BED	6H	5H	5H	5H
AA.IPA.15PeD.BED	6H	5H	5H	4H
AA.IPA.MPD.BED	6H	5H	5H	4H

**Table X.** Cross-hatch Adhesion Values Obtained During Weathering

PU films	Cross-hatch adhesion			
	t = 0 h	t = 480 h	t = 960 h	t = 1440 h
AA.IPA.14BD	5B	5B	5B	5B
AA.IPA.15PeD	5B	5B	5B	5B
AA.IPA.NPG	5B	5B	5B	5B
AA.IPA.MPD	5B	5B	5B	5B
AA.IPA.BED	5B	5B	5B	5B
AA.IPA.NPG.TMP	5B	5B	5B	5B
AA.IPA.16HD.NPG	5B	5B	5B	5B
AA.IPA.MPD.NPG	5B	5B	5B	4B
AA.IPA.16HD.TMP	5B	5B	5B	4B
AA.IPA.MPD.TMP	5B	5B	5B	4B
AA.IPA.16HD.15PeD	5B	5B	5B	5B
AA.IPA.MPD.16HD	5B	5B	5B	5B
AA.IPA.14BD.BED	5B	5B	5B	4B
AA.IPA.15PeD.BED	5B	5B	5B	4B
AA.IPA.MPD.BED	5B	5B	5B	5B

samples: AA.IPA.16HD.TMP and AA.IPA.15PeD.16HD. A noticeable increase in gloss was observed in oligoesters of AA.IPA.NPG. In general, most of the samples retained at least 60% of the gloss. The samples that had a better retention of gloss after accelerated weathering were: AA.IPA.14BD, AA.IPA.NPG, AA.IPA.NPG.TMP, and AA.IPA.MPD.TMP.

Other coating properties such as gouge and scratch hardness, cross-hatch adhesion, and forward impact were also measured during weathering. The results are shown in Tables VIII–XI. The gouge hardness values, Table VIII, show that all the films are able to resist

**Table XI.** Forward Impact Before and After Weathering Exposure

PU films	Forward impact (lb in <sup>-1</sup> )	
	t = 0 h	t = 1440 h
AA.IPA.14BD	39	3
AA.IPA.15PeD	39	2
AA.IPA.NPG	>40	3
AA.IPA.MPD	>40	1
AA.IPA.BED	>40	1
AA.IPA.NPG.TMP	>40	1
AA.IPA.16HD.NPG	>40	1
AA.IPA.MPD.NPG	>40	0
AA.IPA.16HD.TMP	>40	1
AA.IPA.MPD.TMP	>40	1
AA.IPA.16HD.15PeD	>40	1
AA.IPA.MPD.16HD	>40	1
AA.IPA.14BD.BED	>40	1
AA.IPA.15PeD.BED	>40	2
AA.IPA.MPD.BED	>40	2

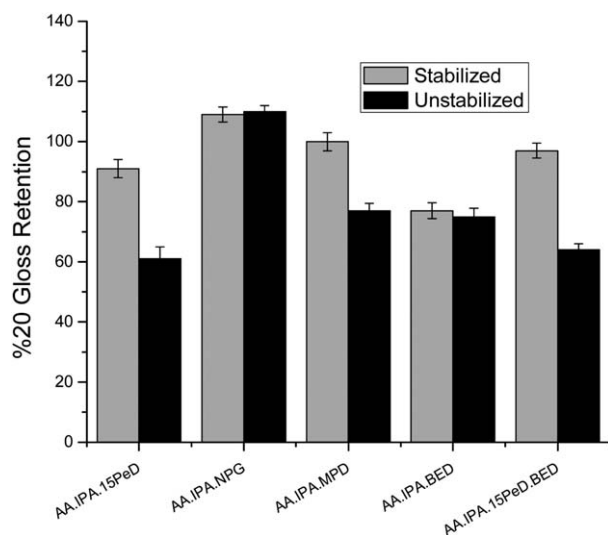


**Figure 3.** Gloss retention ( $20^\circ$ ) of stabilized and unstabilized polyurethane films after 1440 h of weathering.

rupture after 1440 h of exposure. The scratch hardness test, Table IX, shows that some of the samples loose hardness and become softer. These samples include: AA.IPA.14BD, AA.IPA.15PeD, AA.IPA.NPG, AA.IPA.MPD, and AA.IPA.BED. Forward impact, Table X, of all the unstabilized samples after weathering showed poor performance with no values more than  $5 \text{ lb in}^{-1}$  after exposure. This means that the samples deformed easily after an impact due to delamination from the substrate. The cross-hatch adhesion, Table XI, test did not show any variation after weathering.

The addition of UV-absorbers (UVA) and hindered amine light stabilizers (HALS) were also investigated to determine the change in weatherability of the PU films. Unstabilized weathered films, films that displayed haziness or yellowness, were chosen to be tested with the UVA and HALS additives. Figure 3 shows the gloss ( $20^\circ$ ) retention for the selected films. The introduction

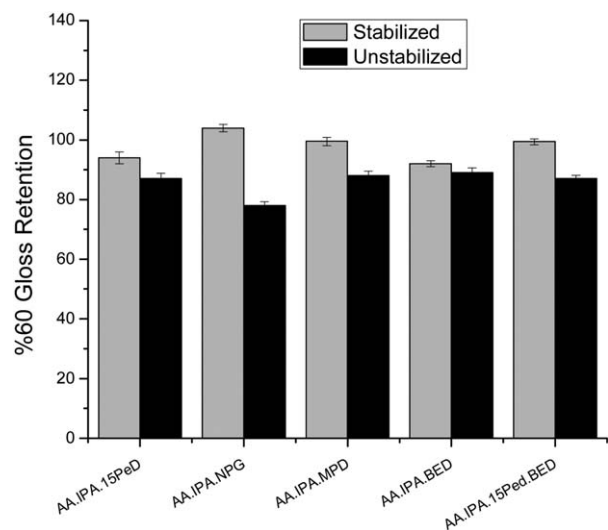


**Figure 4.** Gloss retention ( $60^\circ$ ) of stabilized and unstabilized polyurethane films after 1440 h of weathering.

**Table XII.** Gouge Hardness of Stabilized Samples During Weathering

PU films	Gouge hardness			
	t = 0	t = 480	t = 960	t = 1440
	h	h	h	h
AA.IPA.15PeD.TU	6H	4H	3H	3H
AA.IPA.15PeD.BED.TU	6H	H	F	F
AA.IPA.BED.TU	6H	2B	H	F
AA.IPA.NPG.TU	6H	3H	2H	2H
AA.IPA.MPD.TU	6H	H	B	F

**Table XIII.** Scratch Hardness of Stabilized Samples During Weathering

PU films	Scratch hardness			
	t = 0	t = 480	t = 960	t = 1440
	h	h	h	h
AA.IPA.15PeD.TU	6H	4B	4B	4B
AA.IPA.15PeD.BED.TU	6H	2B	2B	2B
AA.IPA.BED.TU	5H	3H	F	2B
AA.IPA.NPG.TU	F	F	F	F
AA.IPA.MPD.TU	6H	3B	2B	F

of UVA and HALS increased gloss retention by about 20–30%. It is interesting to note the differences between stabilized and unstabilized samples according to the  $20^\circ$  and  $60^\circ$  gloss retention, adhesion, and hardness. The  $20^\circ$  gloss measurements showed noticeable differences between stabilized and unstabilized PU films. On the other hand, the  $60^\circ$  gloss measurements were less sensitive to the differences between the different chemical structures, Figure 4. Another marked difference between stabilized and unstabilized films was the gouge and scratch hardness. Stabilized films were softer than the unstabilized films after 1440 h of weathering. The gouge hardness, scratch hardness, and cross-hatch adhesion for the stabilized films are shown in Tables XII–XIV.

Infrared spectroscopy is a common technique used to monitor chemical changes occurring during weathering, and as such all PU films were monitored by FTIR during weathering. All the PU films show a similar pattern. A representative spectrum is given in Figure 5. Strong absorptions bands were observed at 1680 and

**Table XIV.** Cross-Hatch Adhesion of Stabilized Samples During Weathering

PU films	Cross-hatch adhesion			
	t = 0	t = 480	t = 960	t = 1440
	h	h	h	h
AA.IPA.15PeD.TU	5B	5B	5B	5B
AA.IPA.15PeD.BED.TU	5B	5B	5B	5B
AA.IPA.BED.TU	5B	5B	5B	5B
AA.IPA.NPG.TU	5B	5B	5B	5B
AA.IPA.MPD.TU	5B	5B	5B	5B



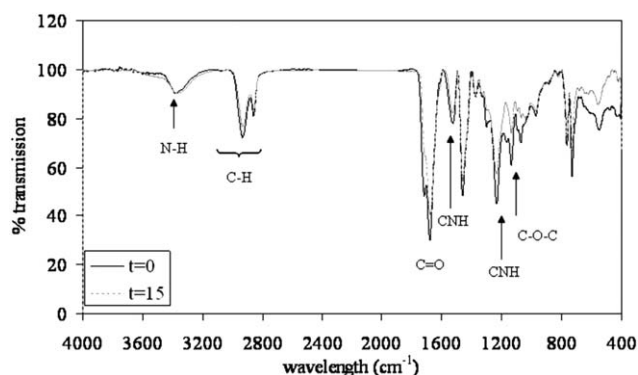


**Figure 5.** Representative FTIR spectrum of polyurethane films before and after 15 days of hydrolysis.

1720  $\text{cm}^{-1}$  ( $\nu(\text{C}=\text{O})$  stretching of H-bonded and free carbonyl groups), 1460  $\text{cm}^{-1}$  ( $-\text{CH}-$  deformation of methylene groups), 1240  $\text{cm}^{-1}$  ( $\nu(\text{C}-\text{N}) + \delta(\text{NH})$ , H-bonded), 730  $\text{cm}^{-1}$  (aromatic ring bending mode). Some other absorptions are observed at 3390  $\text{cm}^{-1}$  ( $\nu(\text{N}-\text{H})$ ), 2940  $\text{cm}^{-1}$  ( $\nu(\text{C}-\text{H})$ ), 1540  $\text{cm}^{-1}$  ( $\nu(\text{C}-\text{N}) + \delta(\text{N}-\text{H})$ , H169 bonded and free), 1140  $\text{cm}^{-1}$  ( $\nu(\text{C}-\text{O}-\text{C})$ ), and 770  $\text{cm}^{-1}$  (out of plane bending vibration of four adjacent hydrogen on aromatic ring). Similar to the FTIR of the hydrolysis of PU films the disappearance of the 1720  $\text{cm}^{-1}$  absorption band confirms the hydrolysis of free carboxyl acid groups (end-groups). Additionally, the disappearance of the urethane bands at 1240 and 1540  $\text{cm}^{-1}$  and the increase in the  $-\text{OH}$  absorption region confirm the degradation of the urethane crosslink and the ester groups during weathering.

The changes in the area under a specific band were used to measure the relative concentration of one functional group with respect to another. The  $-\text{CH}-$  peak is usually preferred for comparison because this peak can be related to the amount of material left or thickness of the film.<sup>12,13</sup> Figure 6 shows the relative concentration of  $-\text{OH}$  and  $-\text{NH}-$  groups on the

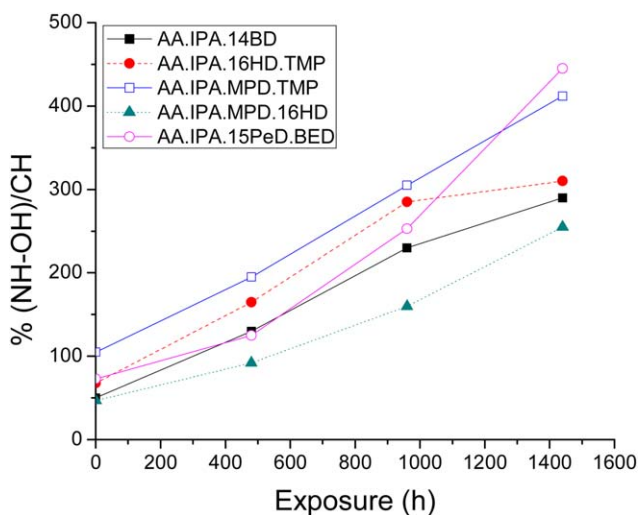


**Figure 6.** Percent increase of the ratio of (NH—OH) area (3600–3100  $\text{cm}^{-1}$ ) to the  $-\text{CH}-$  area (3020–2780  $\text{cm}^{-1}$ ). [Color figure can be viewed in the online issue, which is available at wileyonlinelibrary.com.]

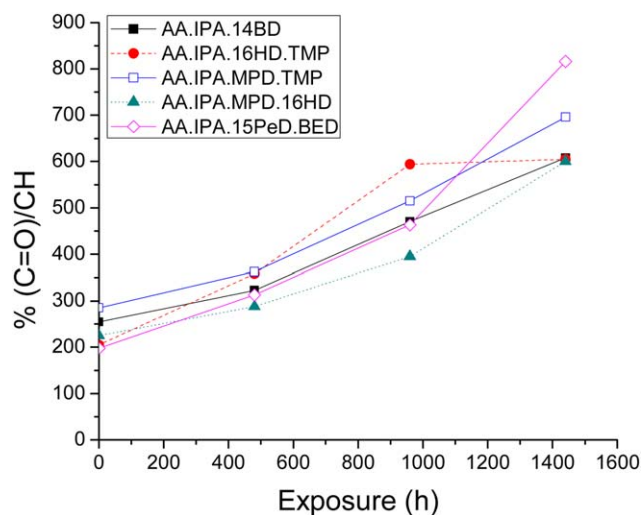


**Figure 7.** Percent increase of the ratio of carbonyl ( $\text{C}=\text{O}$ ) area (1830–1570  $\text{cm}^{-1}$ ) to the  $-\text{CH}-$  area (3020–2780  $\text{cm}^{-1}$ ). [Color figure can be viewed in the online issue, which is available at wileyonlinelibrary.com.]

3600–3100  $\text{cm}^{-1}$  region with respect to the  $-\text{CH}-$  peak on the 3020–2780  $\text{cm}^{-1}$  during weathering exposure (h) for selected samples. Figure 7 shows the relative concentration of carbonyl ( $\text{C}=\text{O}$ ) groups on the 1830–1570  $\text{cm}^{-1}$  region with respect to the  $-\text{CH}-$  groups on the 3020–2780  $\text{cm}^{-1}$  during weathering. The rates of peak appearance (increase in concentration) of the  $\text{OH}-\text{NH}$  region and  $\text{C}=\text{O}$  region with respect to the methylene groups left were obtained from the slopes of lines in Figures 6 and 7. The rates of appearance for all the samples are shown in Table XV.

**Table XV.** Rates of Appearance of the (NH—OH) Groups and ( $\text{C}=\text{O}$ ) Groups with Respect to  $-\text{CH}-$  Groups During Weathering

Samples	Rate $\times 10^3$ % (NH—OH)/day (3600–3100 $\text{cm}^{-1}$ )	Rate $\times 10^3$ % ( $\text{C}=\text{O}$ )/day (1830–1575 $\text{cm}^{-1}$ )
AA.IPA.14BD	173	246
AA.IPA.15PeD	145	190
AA.IPA.NPG	86	36
AA.IPA.MPD	131	180
AA.IPA.BED	369	169
AA.IPA.NPG.TMP	110	195
AA.IPA.16HD.NPG	120	203
AA.IPA.MPD.NPG	186	361
AA.IPA.16HD.TMP	185	292
AA.IPA.MPD.TMP	225	309
AA.IPA.16HD.15PeD	146	238
AA.IPA.MPD.16HD	151	268
AA.IPA.14BD.BED	269	460
AA.IPA.15PeD.BED	262	376
AA.IPA.MPD.BED	288	304

## DISCUSSION

To relate small molecule behavior that is reaction pathways, mechanisms, and rates to solid polymeric materials is not an easy task. Huge differences in mobility and the environment which surrounds albeit the same chemical groups contributes to a lack of correlation between small model compounds and the actual polymeric material. For polyesters, hydrophobicity/hydrophilicity,  $T_g$ , crosslink density, end group-effects, interactions with pigments, fillers, and other additives all can contribute to the differences in model compounds studies and observed degradation in the solid polymeric films. In previous studies, the hydrolytic stability of oligoesters were investigated using a water/acetone solution.<sup>2-4</sup> Because end group effects was such an issue for the flexible monomers, it was thought that end-capping of the oligoesters with a monoisocyanate would be a better model for oligoester behavior as soft segments in polyurethanes.

The water/acetone system provided an ideal environment wherein large amounts of water surrounded each molecule in the system, providing a constant water concentration throughout the experiment. Intermolecular catalysis through end-group effects was not considered as part of this analysis since intermolecular interactions in polyesters are relatively weak.<sup>14</sup> In addition, diluted systems also minimize the interaction between molecules. Concentrated systems have the disadvantage of being time-dependent<sup>15</sup>; thus as the hydrolytic reaction takes place, the formation of carboxyl-acid groups increases and has an impact not only in the molecule itself (intramolecular catalysis) but also in the surrounding molecules, favoring intermolecular catalysis. In addition, dissolving the oligomer in acetone helped the molecule to disentangle, allowing the attack of water at different positions in the molecule.

Chain scission at different points along the polyurethane network has been previously reported: random chain scission and end-group scission. Several studies have shown the presence of both scenarios: random chain scission and autocatalysis by hydrogen ( $H^+$ ) or carboxyl ( $COO^-$ ) ions produced by the hydroxyl or carboxyl acid end-groups. When random chain scission is present, weight gain is expected. The release of a molecule during random chain scission could only happen when two ester groups located in between crosslink points are hydrolyzed. This event breaks the molecules at nearby points and could potentially release a small molecule.<sup>16,17</sup> The film emersion data roughly correlates with model urethane oligoester solution data. Relative ordering is not exact, but the systems which show the highest rate of weight loss also show the highest rate of hydrolysis (AA.IPA.BED and AA.IPA.15PeD.BED), and the low weight loss and low rate constant oligoester follow the same general trend. The differences can be attributed to stronger acid, crosslink density, and the other factors previously discussed (*supra vide*).

Although the goal of this article was not to deconvolute the degree of hydrolysis and free radical photo-oxidation during weathering it is known that photo-oxidation produces acids which can participate in hydrolysis reactions. Therefore, it was of interest to investigate the surface in terms of loss of gloss<sup>11</sup>

with and without an exterior stability package and look at a couple basic coating tests. The coating tests were augmented by IR data which was measuring the generation of hydrolysis products through-out the film cross-section.

As expected, results indicated that unstabilized PU films were susceptible to the degradation effects (sunlight, moderate temperature, and water), causing extensive deterioration. However, the addition of UVA and HALS stabilizers increased the gloss retention for all the PU films studies (see Figures 3 and 4) compared to the unstabilized. This is consistent with previously reported results with photo-oxidation.<sup>3</sup> An increase ( $>100\%$ ) in the  $20^\circ$  gloss values (see Figure 2) during the weathering exposure was observed for one of the systems tested. This also has been observed by several authors in similar systems.<sup>18,19</sup> Only AA.IPA.14BD, and AA.IPA.NPG showed this particular behavior for  $60^\circ$  gloss. These samples were characterized by having low hydrolysis rates. Consequently, the high gloss retention may be associated with the onset of the hydrolysis, which resulted in plasticization by water instead of erosion.

The coating properties measured and in particular the hardness tests (see Tables XII and XIII), showed that the results qualitatively followed the hydrolysis rate of the model urethane terminated oligoesters. The hydrolysis resistant oligoesters (AA.IPA.15PeD and AA.IPA.NPG) lost hardness slowly, whereas, the others which had higher hydrolysis rates lost more hardness with increasing exposure times.

A correlation analysis was performed for gloss or the IR measured hydrolysis of the films and the model urethane terminated oligoesters. As anticipated, a poor correlation was observed for  $20^\circ$  and  $60^\circ$  gloss ( $R = 0.53$  and  $0.15$ ) as shown in Figures 8 and 9, respectively. This was expected since the surface activity is expected to be photo-oxidative dominated and not hydrolysis driven degradation. Photo-degradation during weathering could have contributed to the differences between the correlation of the hydrolysis and weathering results. This being the case, the

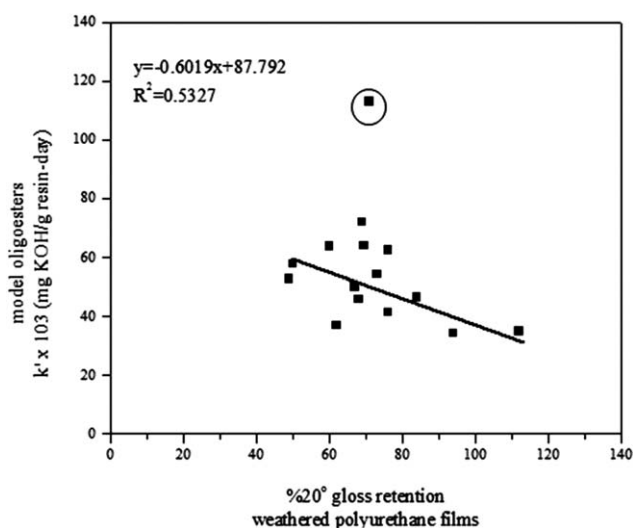


**Figure 8.** Correlation between hydrolysis of end-capped oligoesters and  $20^\circ$  gloss retention (%). Excluded point: AA.IPA.BED.

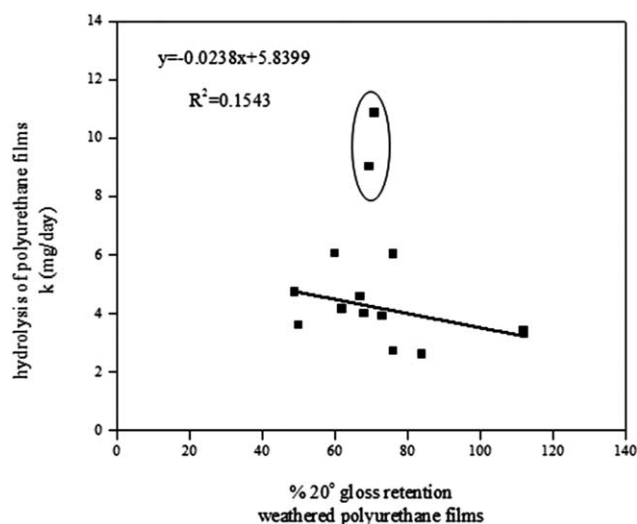


**Figure 9.** Correlation between hydrolysis of polyurethane films and 20° gloss retention (%). Excluded point: AA.IPA.BED and AA.IPA.BED.15PeD.

lowest correlation was observed for the PU films containing an unsaturation in the backbone, namely, AA.IPA.BED and AA.IPA.BED.15PeD. It is reasonable to assume that the butene-diol (BED) caused the photo-oxidative degradation pathway to dominate.

Figure 10 shows the correlation ( $R = 0.78$ ) between the  $-\text{OH}$ ,  $-\text{NH}-$  groups in the FT-IR of the weather films, and the hydrolysis measured by weight loss of polyurethane films immersed in acid solution. The correlation suggests that the solution behavior of the urethane terminated oligoesters models the hydrolysis behavior of the solid thermoset films. Correlation analysis, Figure 11, shows that the correlation ( $R = 0.51$ ) between the area increase in the  $3600\text{--}3100\text{ cm}^{-1}$  region of the weathered films, corresponding to the  $-\text{OH}$ ,  $-\text{NH}-$  groups and the hydrolysis of end-capped oligoesters. Although not

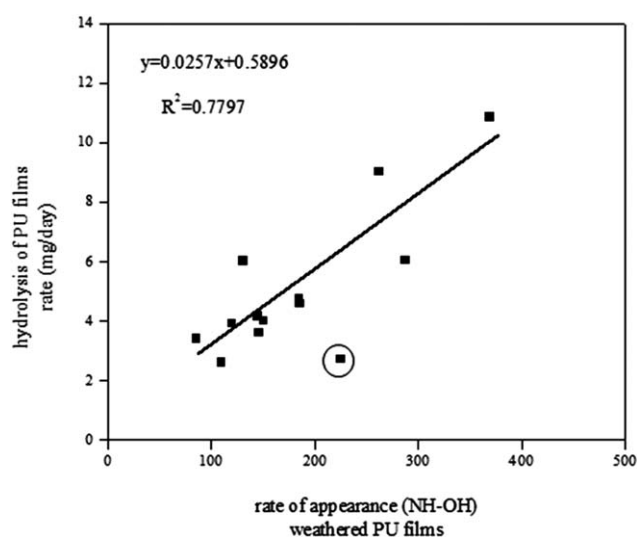


**Figure 10.** Correlation between the hydrolysis of PU films and the rate of increase in the  $\text{NH}-\text{OH}$  area during weathering. Excluded point: AA.IPA.MPD.TMP.

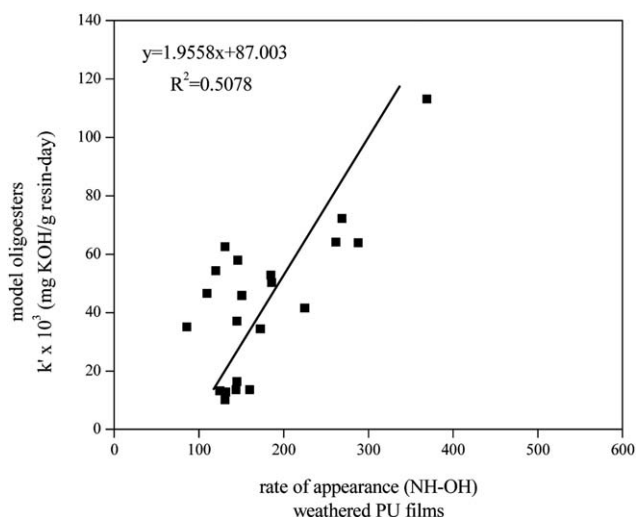


**Figure 11.** Correlation between the hydrolysis of end-capped oligoesters and the rate of increase in the  $\text{NH}-\text{OH}$  area during weathering.

quite as good of a fit as the acid immersion, there still is a perceivable correlation of the hydrolytic stability of the urethane terminated oligoesters. This is understandable, since free radical processes are in competition with hydrolysis. However, it should also be noted that photo-oxidation creates acids which catalyze hydrolysis. Although it certainly is not a 1 : 1 correlation, it can be surmised that even in relatively neutral pH (at least for external exposure, see Table III), more than half of the degradation that is associated with exterior weathering (this particular cycle) is linked to the hydrolytic stability of the oligoester. Therefore, the solution testing of urethane oligoester has some validity as a model for predicting the performance of thermoset urethane films especially in areas prone to acid rain.

To the best of our knowledge, this is the first time a correlation between hydrolysis of oligoesters and weathering of polyester-urethane film has been done. The reasonable correlation obtained between hydrolysis and weathering is an indication of the potential of this type of experiment. Weathering experiments are expensive and time consuming. Thus, a good approximation of the weathering performance of outdoor coatings can be obtained by a simple and inexpensive hydrolysis of model oligoester compounds (end-capped).

## CONCLUSIONS

The hydrolytic stability of a series of urethane terminated oligoesters comprised of three and four different monomers was evaluated, and used as models for thermoset urethane films. Films containing BED showed different trends to the rest of PU films due to the unsaturation present in the backbone. Some of the coating properties followed the same trends as the hydrolysis rates of the model urethane terminated oligoesters. For an acidic environment, there was good correlation with the urethane coating degradation and model urethane terminated oligoesters. For the neutral pH, there was a reasonable correlation between the urethane films and model system. The hydrolysis of end-capped oligoesters can be potentially used to predict the weathering of PU films.

## REFERENCES

1. Wicks, Z. W.; Jones, F. N.; Pappas, S. P.; Wicks, D. A. *Organic Coatings: Science and Technology*, 3rd ed.; Wiley-Interscience: Hoboken, NJ, **2007**.
2. Johnson, A. H.; Wegner, J.; Soucek, M. D. *Eur. Polym. J.* **2004**, *40*, 2773.
3. Soucek, M. D.; Johnson, A. H.; Meemken, L. E. *Macromol. Chem. Phys.* **2004**, *205*, 35.
4. Soucek, M.; Johnson, A. *J. Coat. Technol. Res.* **2004**, *1*, 111.
5. Seubert, C. M.; Nichols, M. E.; Cooper, V. A.; Gerlock, J. L. *Polym. Degrad. Stab.* **2003**, *81*, 103.
6. Turpin, E. T. *J. Paint Tech* **1975**, *47*, 40.
7. Payne, K.; Jones, F. N.; Brandenburger, L. W. *J. Coat. Technol.* **1985**, *57*, 36.
8. Newman, M. S. *Steric Effects in Organic Chemistry*; Wiley: New York, **1956**.
9. Klemann, B. M. *Mater. Test. Prod. Technol. News (ATLAS)* **2005**, *35*, 1.
10. Bauer, D. R. *Polym. Degrad. Stab.* **2000**, *69*, 307.
11. Wernstahl, K. M.; Carlsson, B. J. *Coat. Technol.* **1997**, *69*, 39.
12. Decker, C.; Masson, F.; Schwalm, R. *Polym. Degrad. Stab.* **2004**, *83*, 309.
13. Bauer, D. R. *J. Coat. Technol.* **1994**, *66*, 57.
14. SITA Technology Limited. *Waterborne and Solvent-based Surface Coating Resins and their Applications*; Wiley: Chichester, 1998.
15. Connors, K. A. *Chemical Kinetics: The Study of Reaction Rates in Solution*; VCH: New York, **1990**.
16. Mortaigne, B.; Bellenger, V.; Verdu, J. *Polym. Networks Blends* **1992**, *2*, 187.
17. Bellenger, V.; Ganem, M.; Mortaigne, B.; Verdu, J. *Polym. Degrad. Stab.* **1995**, *49*, 91.
18. Yang, X. F.; Vang, C.; Tallman, D. E.; Bierwagen, G. P.; Croll, S. G.; Rohlik, S. *Polym. Degrad. Stab.* **2001**, *74*, 341.
19. Belder, E.; Koldijk, F. *Surf. Coat. Int.* **1996**, *10*, 449.